University of Baghdad
College of Engineering
JOURNAL OF ENGINEERING

Journal of Engineering

journal homepage: www.joe.uobaghdad.edu.iq

Volume 29 Number 11 November 2023

Optimum Reinforcement Depth Ratio for Sandy Soil Enhancement to Support Ring Footing Subjected to a Combination of Inclined-Eccentric Load

Jumana Yousif Mohammed Ali[1,*], A'amal A.H. Al-Saidi[2]

Department of Civil Engineering, College of Engineering, University of Baghdad, Baghdad, Iraq.
jumana.mohammed2001m@coeng.uobaghdad.edu.iq[1] , dr.aamal.al-saidi@coeng.uobaghdad.edu.iq[2]

ABSTRACT

This work investigates the impacts of eccentric-inclined load on ring footing performance resting on treated and untreated weak sandy soil, and due to the reduction in the footing carrying capacity due to the combinations of eccentrically-inclined load, the geogrid was used as reinforcement material. Ring radius ratio and reinforcement depth ratio parameters were investigated. Test outcomes showed that the carrying capacity of the footing decreases with the increment in the eccentric-inclined load and footing radius ratio. Furthermore, footing tilt and horizontal displacement increase with increasing the eccentricity and inclination angle, respectively. At the same time, the increment in the horizontal displacement due to the inclined load reduces with increasing the eccentricity ratio.
The results also revealed that the optimum radius ratio under eccentrically-inclined load is n=0.30, the optimum depth ratio is U/B=0.50, and at the optimum depth ratio and with eccentricity ratio of 0.16 and for the inclination angles of 5, 10, 15 the improvement in the carrying capacity was by (115.1%, 126.5%, and 131.5%) for the inclination angles of respectively.

Keywords : Eccentric-inclined load, Ring footing, Reinforcement, Reinforcement depth ratio.

*Corresponding author
Peer review under the responsibility of University of Baghdad.
https://doi.org/10.31026/j.eng.2023.11.06

Article received: 03/01/2023
Article accepted: 06/02/2023
Article published: 01/11/2023

نسبة العمق المثلى للتسليح لتحسين تربة رملية تدعم أساس حلقي معرض لأحمال مائلة وغير متمركزة

جمانة يوسف محمد علي[1]،*، امال عبد الغني السعيدي[2]

قسم الهندسة المدنية, كلية الهندسة، جامعة بغداد، بغداد، العراق

الخلاصة

يبحث هذا العمل في تأثيرات الحمل المائل الغير متمركز على أداء الأساس الحلقي المرتكز على تربة رملية ضعيفة مسلحة وغير مسلحة ، وبسبب انخفاض قدرة تحمل الاساس نتيجة لدمج الاحمال المائلة الغير متمركزة ، تم تسليح التربة بواسطة المشبكات. تم فحص نسبة نصف قطر الأساس وعمق طبقة التسليح الاولى. أظهرت نتائج الاختبار أن قابلية تحمل الأساس تتناقص مع الزيادة في الحمل المائل الغير متمركز ونسبة نصف قطر الاساس. علاوة على ذلك، يزداد ميلان الأساس والإزاحة الأفقية مع زيادة اللاتمركز وزاوية الميل على التوالي ، وفي نفس الوقت ، تقل الزيادة في الإزاحة الأفقية بسبب الحمل المائل مع زيادة نسبة اللاتمركز. أظهرت النتائج أيضًا أن نسبة نصف القطر المثلى تحت الحمل المائل الغير متمركز هي $n = 0.30$ وأن نسبة العمق المثلى هي $U / B = 0.50$ وعند نسبة العمق المثلى ونسبة اللاتمركز 0.16 ولزوايا الميل 10،5 15 ، كان التحسن في القدرة الاستيعابية بنسبة (115.1٪ ، 126.5٪ ، 131.5٪) على التوالي.

الكلمات المفتاحية: احمال غير متمركزة ومائله، أساس حلقي، تسليح, نسبة عمق التسليح

1. INTRODUCTION

Ring or Hollow circular footings provide various benefits and advantages over circular footings, such as reduced material volume and construction expense. Ring or hollow circular foundations are typically utilized in tall circular buildings such as bridge piers, water storage tanks, silos, transmission towers, oil containers, etc. **(Boushehrian and Hataf, 2003, 2008; Al-sumaiday and Al-tikrity, 2013)**. All of them are axisymmetric structures. These foundations are often exposed to vertical pressures from the superstructure and horizontal stresses from wind pressure acting on the structure. Furthermore, the eccentricity of the resultant load's point may be caused by the position of the horizontal load (centroid) anywhere along the structure height**. (Sharma and Kumar, 2018; Bachay and AL-Saidi, 2022; Al-Mosawe et al., 2008).**

Many soil improvement techniques have been adopted in soil engineering practice to enhance soil behavior and minimize the settlement of the foundation. Recently, it has been discovered that reinforcing materials such as geotextile, geosynthetics, and geogrid increase the value of UBC (ultimate bearing capacity), and this is due to their open grid structure, which allows bonding between geogrid and soil; geosynthetic materials have high tensile strength at low strain, a long operating life, and are lightweight **(Shukla et al., 2009; Al-Mosawe et al., 2010; Cicek, 2012)**

Many other researchers were done to explore and discuss the behavior of soil reinforcement, such as **(Xu et al., 2020; Kolay and Kumar, 2020; Das and Samadhiya, 2020; Al-Jeznawi and Al-Azzawi, 2021; Jawad and Shakir, 2021;).**

(Moayed et al., 2012) evaluate the ring footing carrying capacity resting on two layered soils using finite element analysis; the first layer is clay, and the second is cohesionless soil. The impact of the radii ratio and the thickness of the clay layer was studied, and the results showed that the carrying capacity of the footing decreased as the ring radii ratio increased. Also, as the depth of the clay layer increases, the carrying capacity decreases gradually.

The performance of a model strip foundation resting on dry sand and exposed to the action of eccentric, inclined loads with varied embedment ratios (D/B) varies from (0-1), has been investigated by **(Ali, 2016)** that used finite element software (Plaxis 3D Foundation). The analysis shows that the carrying capacity of a strip foundation reduces remarkably with the increment of eccentricity ratio (e/B) and the inclination angle (α). As the model footing is positioned at a specific depth beneath ground level, the impacts of overturning and sliding related to eccentrically inclined load are reduced.

(Fazel and Bazaz, 2020) proposed the failure envelope approach to predict the behavior of ring footings exposed to inclined and eccentric loading combinations. Several parameters were investigated, such as load inclination angle, load eccentricity, and ring radius ratio. Circular footing and ring footings with various ring radius ratios (n=0.2, 0.4, 0.6) were also investigated. The research outcomes showed that when the load inclination increases, the permissible eccentricity decreases, and in the same way as the eccentricity, the acceptable angle decreases. It is observed that n=0.4 is the optimum value for ring footing under a combination of eccentric and inclined loads.

(Kadhum and Albusoda, 2021) examined experimentally the behavior of the ring and circular footings subjected to eccentric loading over sandy soil. The results showed an increase in carrying capacity and a decrease in settlement for the ring footing compared to the circular footing under the same condition, which makes the ring footing more cost-effective compared with a circular one. Also, the results showed that the differential settlement increases as eccentricity increases due to changing the bearing pressure under the footing.

This research aimed to investigate ring footing performance under eccentrically inclined load resting on weak sandy soil, and because ring footing has been increasingly used in various structures in recent years, it was also important to study an improvement method since the footing is over weak soil and is subjected to eccentrically inclined load. Soil reinforcement was used as an improvement method since reinforcement materials such as geogrid are among the most reliable and cost-effective techniques in recent years.

1.1 Soil Properties

The soil is poorly graded sand and was classified according to USCS. The sample's grain distribution size was evaluated using ASTM D422-63, as shown in **Fig. 1**. The soil was brought from the Karbala governorate in Iraq. The used soil was sieved on sieve No.10., and dried in the air. The soil sample properties are given in **Table 1.**

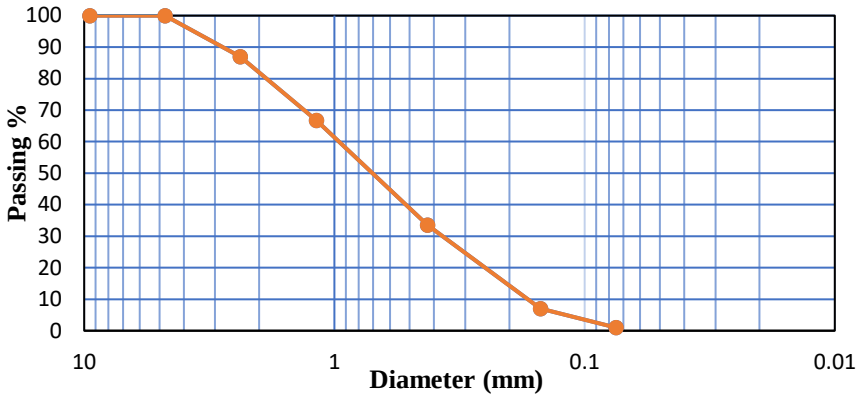

Figure 1. Soil grain size distribution

Table 1. Soil properties

Property	Specification	Result
classification	ASTM D 2487	SP
Coefficient of curvature c_c	ASTM D 422	5.5
Coefficient of uniformity c_u	ASTM D 422	0.94
D60		0.93
D50		0.70
D30		0.39
D10		0.17
Gs	ASTM D 854	2.65
Direct shear, loose sand Dr=30%	ASTM D 3080	$\varphi = 32°$
γ_{dmin}	ASTM D 2049-69	14.5 KN/m^3,e_{max}=0.82
Dry unit weight in the test of Dr=30%	ASTM D 2049-69	$\gamma_d = 15.1\ kN/m^3$, e=0.75

1.2 Reinforcement Properties

The geogrid was used as reinforcement material; its properties are illustrated in **Table 2.**

Table 2. Reinforcement properties (product specification)

Property	Data	Property	Data
Mesh type	rectangle	Roll width	1.2m
Rib thickness	1.5 mm	Roll length	30m
Rib width	1.6mm	Elastic modulus	0.26 Gpa
Junction thickness	1.8 mm	Tensile strength	2.25 Mpa

1.3 Testing Setup

A physical model carried out the experimental work to investigate the behavior of ring footings with different radius ratios n (where $n=R_{in}/R_{out}$, Rin=inner footing radius, Rout= outer footing radius)(n=0.25, n=0.30, n=0.35, n=0.40, 0.45) and all footings with outer diameter 100 mm, which rested on reinforced and unreinforced sandy soil. The manufactured physical model is shown in **Fig. 2** and consists of a container box with dimensions of 60*60 cm and 50 cm in height and with one face of the glass. The box has a loading frame connected to it, as shown in **Fig. 2**, and consists of an electrical jack of 2 tons that works on a 12 V and 15 A battery. To adjust the loading rate, a selector was added. A voltage-stabilizing card maintains a constant electrical current while not affecting the loading rate. Finally, before the tests, the battery is charged using a battery charger to apply eccentrically-inclined loading at a constant.

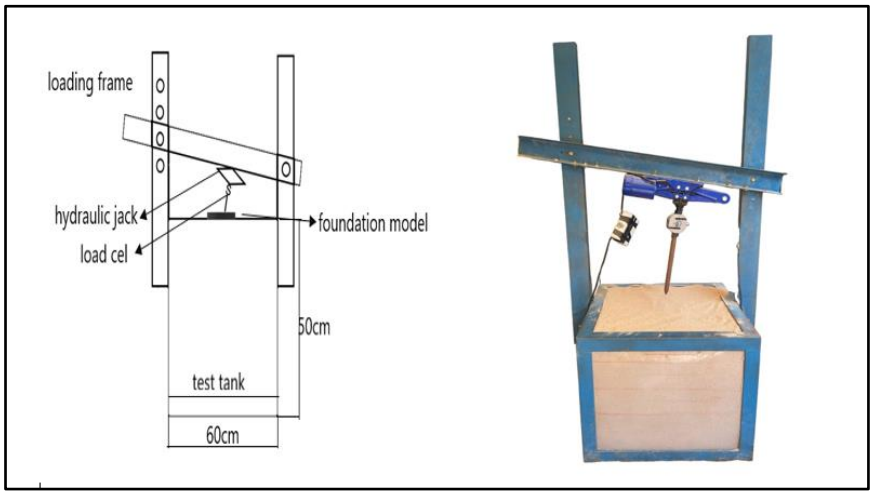

Figure 2. The used physical model

The load was measured by using load cell SI400 with a 1-ton capacity, which is connected to a digital indicator to display the data; a dial gauge with a 25 mm capacity was used to estimate the horizontal displacement, and two dial gauges with a 50 mm capacity were used to estimate the vertical settlement on the edges of the footing. These devices were placed and secured to the footing by using a magnetic holder**.**

2. TESTING PROCEDURE

2.1 Soil Preparation

The raining technique was used to fill the box with sand and to achieve a relative density of 30%, with a dry unit weight of γ=15.1 kN/m^3. The mechanical system that was used is similar to that used by **(Bieganousky and Marcuson, 1976)** and many other researchers such as **(Al-Mhaidib, 1999; Al-Busoda and Hussein, 2013; Yadu and Tripathi, 2013; Fakher and Fakhruldin, 2021).** These tests were performed to ensure and control the homogeneity of the sand bed.

2.2 Testing Procedure

The soil is placed in the tank using a hopper. The sand was placed in layers with 10 cm depth to achieve a tank height of 50 cm. After placing each layer, the soil is leveled gently using a sharp tool to ensure no disturbance. After that, the footing is placed in the center of the soil surface, then two dial gauges are placed at the edges of the footing to estimate the vertical settlement, and the third one is placed horizontally on the side to measure the horizontal displacement, then apply the load through the electrical jack according to the test condition with various load inclinations and eccentricities. The eccentricity values were taken as (e/B=0, 0.04, 0.08, 0.16) in a combination of inclination values of (α=0, 5, 10, 15) and centric vertical load.

3. RESULTS AND DISCUSSION

3.1 Footing Radius Ratio

Fifty tests have been carried out on five different radius ratios (n=0.25,n=0.30, n=0.35, n=0.40, n=0.45) where (n= R_{in}/R_{out}, n= radius ratio, R_{in}= inner radius, R_{out}=outer radius) to obtain the optimum radius ratio under a combination of eccentrically-inclined load, the values of eccentricity and inclination were (e/B=0, 0.04, 0.08, 0.16) and (α=0, 5, 10, 15).
Fig. 3 illustrates the relationship between load and settlement ratio S/B % where (S is the vertical settlement, B is the footing outer diameter) for various ring radius ratios under centric-vertical load. The outcomes show that the optimum ring radius ratio under a centric vertical load is 0.4, which is similar to many studies carried out before under different load conditions and soil densities, such as those **(El Sawwaf and Nazir, 2012; Al-Sumaiday and Al-Tikrity, 2013)**.
Figs. 3 to **12** represent the relationship between load and S/B % for ring footing with various ring radius ratios and under different values of eccentrically inclined load.

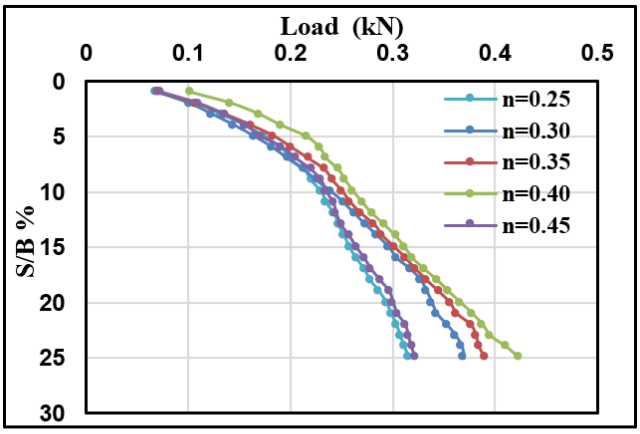

Figure 3. Load-settlement ratio relationship for various ring radius ratios under eccentricallv-inclined load at e=0. α=0.

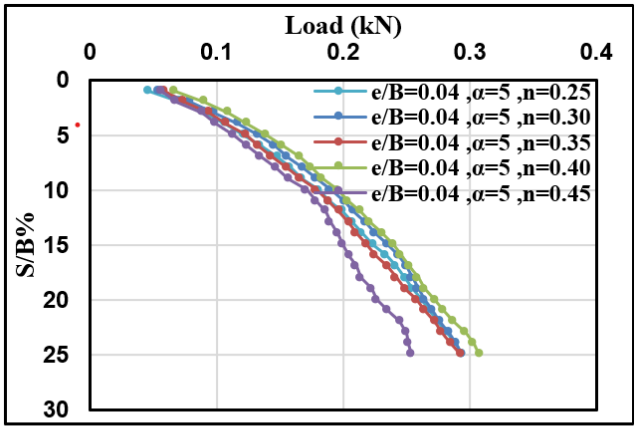

Figure 4. Load-settlement ratio relationship for various ring radius ratios under eccentrically-inclined load at e/B=0.04, α=5.

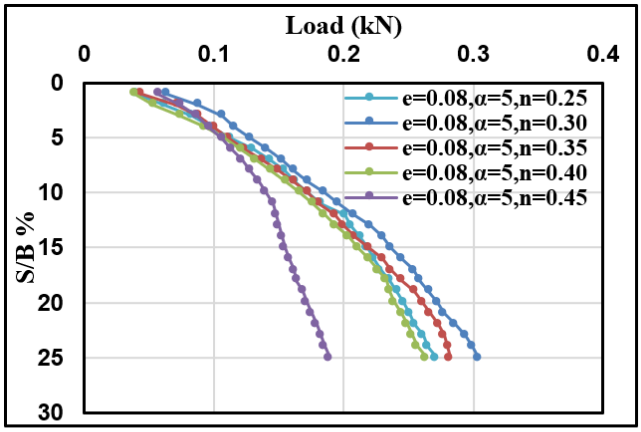

Figure 5. Load-settlement ratio relationship for various ring radius ratios under eccentrically-inclined load at e/B=0.08, α=5.

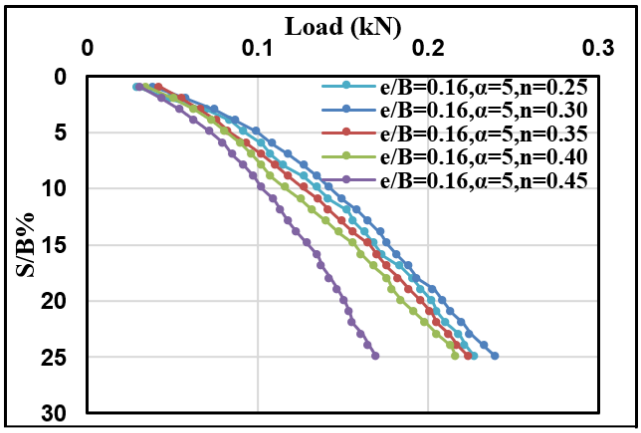

Figure 6. Load-settlement ratio relationship for various ring radius ratios under eccentrically-inclined load at e/B=0.16, α=5.

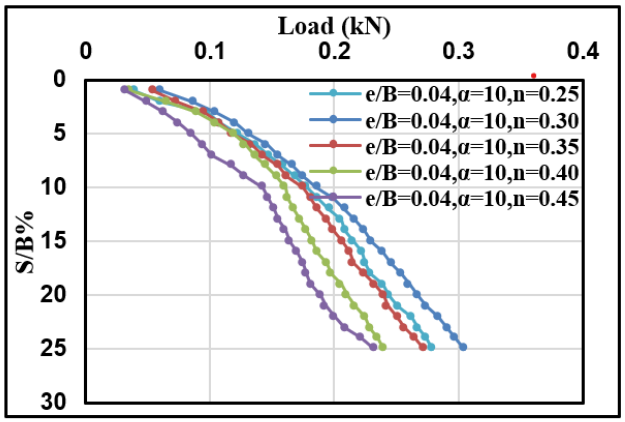

Figure 7. Load-settlement ratio relationship for various ring radius ratios under eccentrically-inclined load at e/B=0.04, α=10.

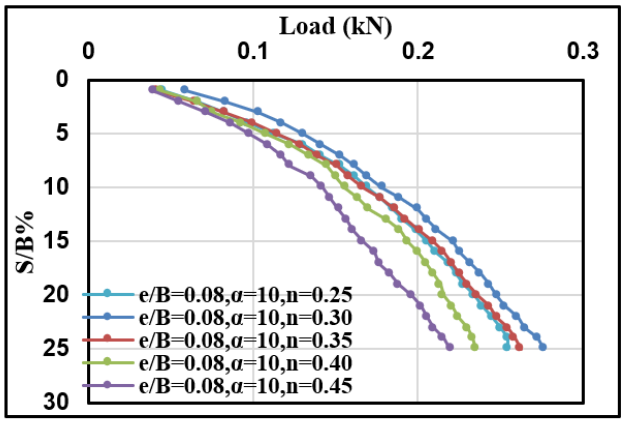

Figure 8. Load-settlement ratio relationship for various ring radius ratios under eccentrically-inclined load at e/B=0.08, α=10.

Fig. 4 shows that the radius 0.4 is the optimum as the eccentricity and inclination values are small. As the eccentricity and inclination increase, the optimum radius ratio tends to be 0.3 **Figs. 5** to **12.** According to the results, in general, the optimum radius ratio for ring footing under an eccentrically inclined load is 0.3 **(Snodi, 2010)** mentioned that footing carrying capacity reaches its maximum value in the range of (0.20-0.40) due to the interaction in the failure wedges that forming under the footing.

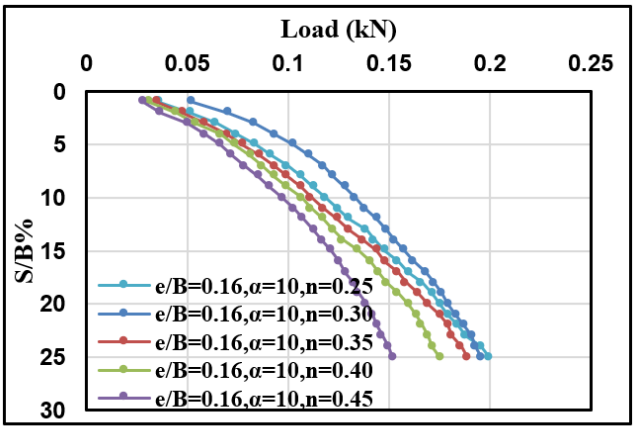

Figure 9. Load-settlement ratio relationship for various ring radius ratios under eccentricallv-inclined load at e/B=0.16. α=10.

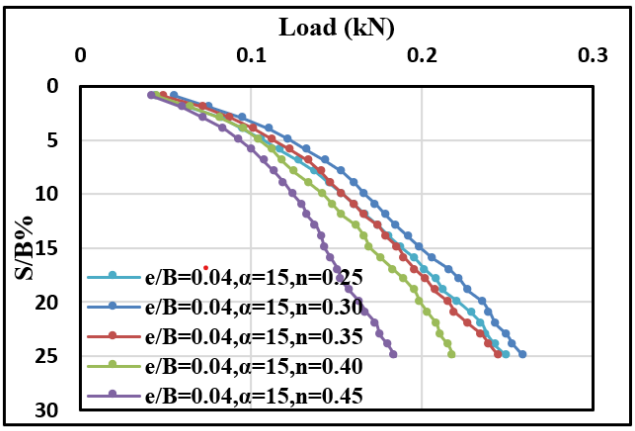

Figure 10. Load-settlement ratio relationship for various ring radius ratios under eccentrically-inclined load at e/B=0.04, α=15.

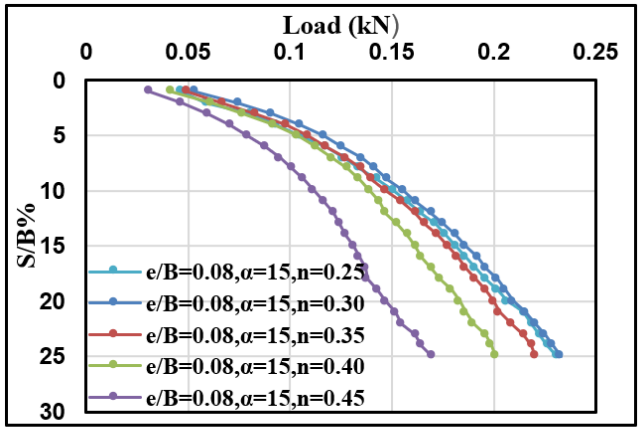

Figure 11. Load-settlement ratio relationship for various ring radius ratios under eccentrically-inclined load at e/B=0.08, α=15.

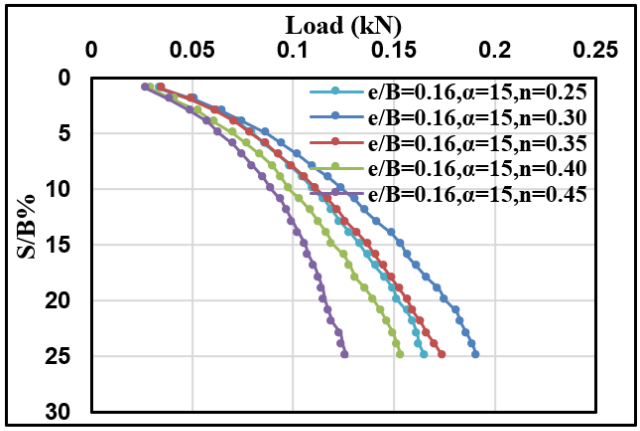

Figure12. Load-settlement ratio relationship for various ring radius ratios under eccentrically-inclined load ate/B=0.16, α=15.

(Patel and Bhoi, 2019) also found that footing carrying capacity decreases with the increase in the ring radius ratio under axial load. **(Fazel and Bazaz, 2020)** approved the reduction of carrying capacity with an increase in radius ratio and found that the optimum value is when n=0.4, and the carrying capacity decreases as the radius ratio increases. This could be explained as a result of reducing the effective area of the footing due to eccentricity, which works on overturning the footing, reducing the contact of the footing with the soil. The outcomes also show that, in general, footing carrying capacity reduced with the increase in the value of the eccentrically-inclined load and is also reduced with increases in the footing ring radius ratio. Also, it was noticed that footing tilt increases as eccentricity increases regarding the load inclination angle.

3.2 Reinforcement First Layer Depth Ratio

To study the effect of the depth of the first layer of reinforcement on enhancing the carrying capacity of the foundation, several laboratory tests were conducted (40 tests) for different

ratios of the depth ratio (U/B=0.25, 0.50, 0.75, 1) where (U is the reinforcement first layer depth, B is the footing outer diameter) under various values of eccentrically- inclined load. **Figs. 13** to **22** show the relationship between the load-settlement ratio (S/B) % for different U/B ratios under various values of eccentrically-inclined load.

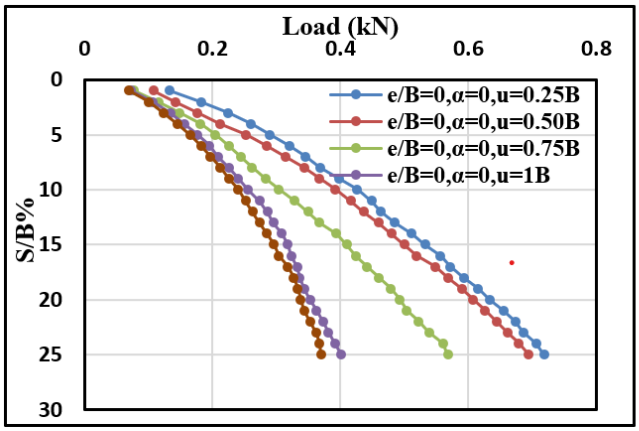

Figure 13. Load-settlement ratio relationship for various reinforcement depth ratios at e/B=0, α=0.

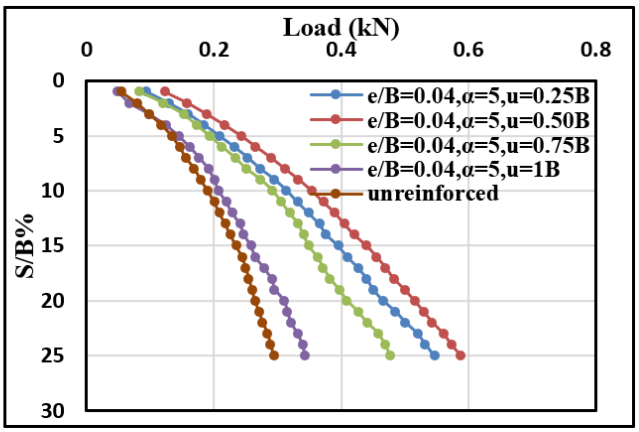

Figure 14. Load-settlement ratio relationship for various reinforcement depth ratios at e/B=0.04, α=5.

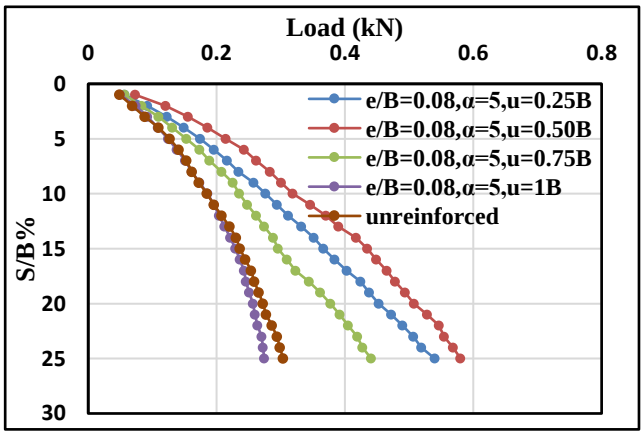

Figure 15. Load-settlement ratio relationship for various reinforcement depth ratios at e/B=0.08, α=5.

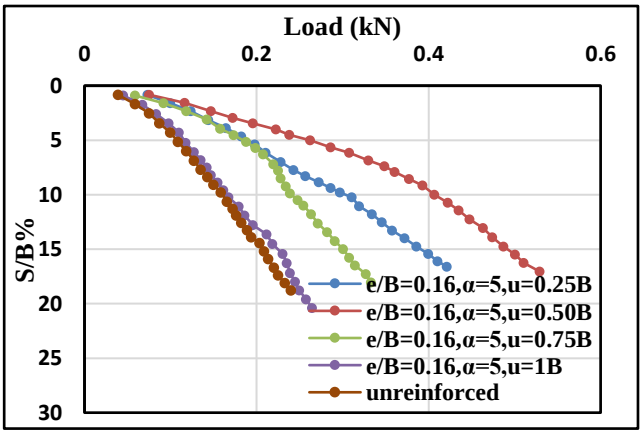

Figure 16. Load-settlement ratio relationship for various reinforcement depth ratios at e/B=0.16, α=5.

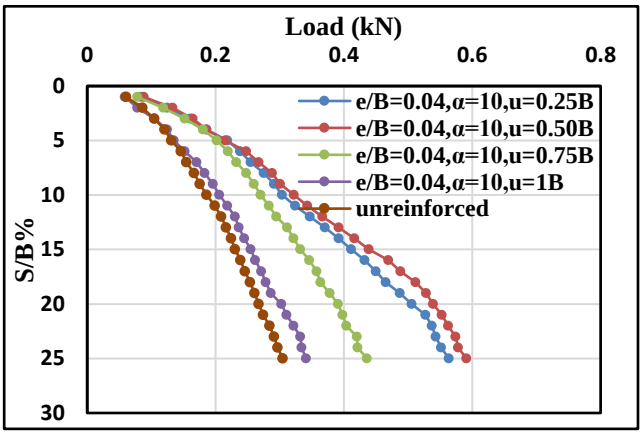

Figure 17. Load-settlement ratio relationship for various reinforcement depth ratios at e/B=0.04, α=10.

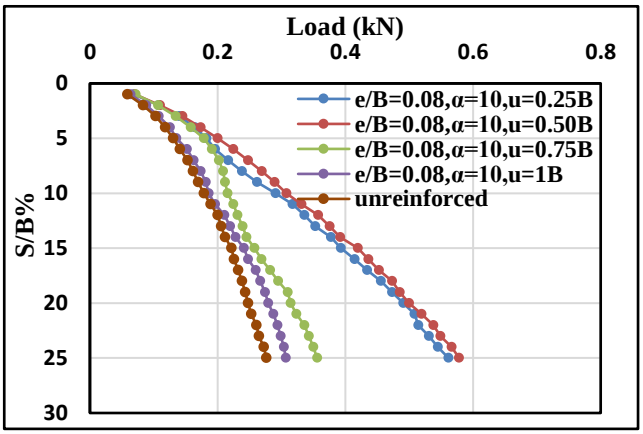

Figure 18. Load-settlement ratio relationship for various reinforcement depth ratios at e/B=0.08, α=10**.**

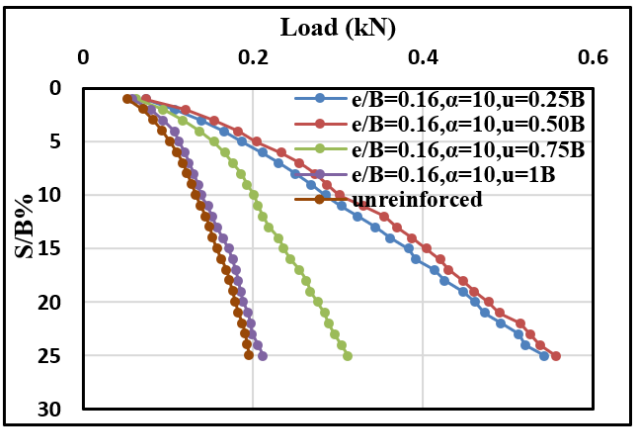

Figure 19. Load-settlement ratio relationship for various reinforcement depth ratios at e/B=0.16, α=10.

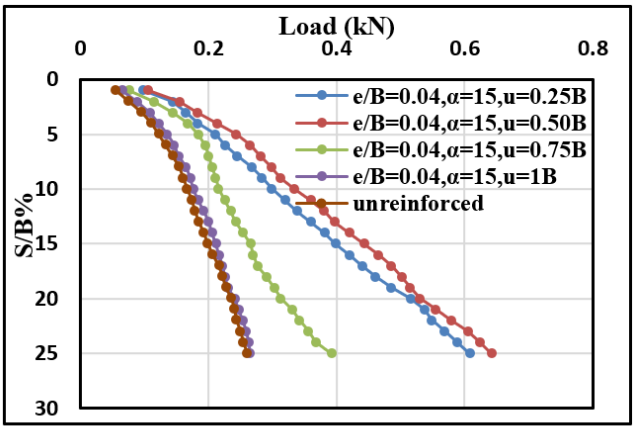

Figure 20. Load-settlement ratio relationship for various reinforcement depth ratios at e/B=0.04, α=15.

The carrying capacity improvement percent IR% is given in **Table 3.** It is calculated as:

$$(IR\%=((load_{(treated)}-load_{(untreated)})/load_{(untreated)})*100) \quad (1)$$

For ring footing under different values of eccentrically- inclined loads and with varying ratios of first layer depth (U/B). The table illustrates the variable carrying capacity improvement percentages with variable depth ratios. This also shows the increase in the improvement percent of the carrying capacity with reinforced soil as the eccentricity and inclination value increase.

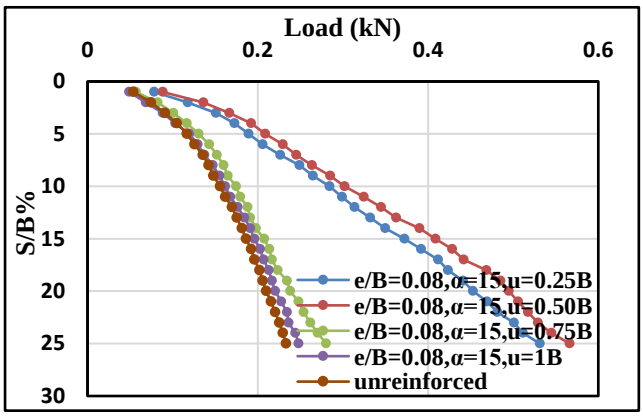

Figure 21. Load-settlement ratio relationship for various reinforcement depth ratios at e/B=0.08, α=15.

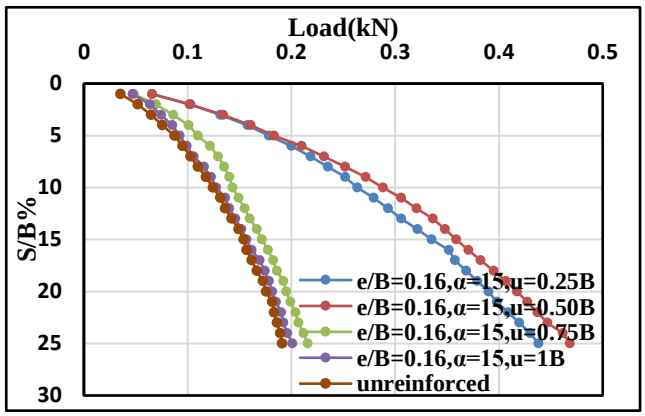

Figure 22. Load-settlement ratio relationship for various reinforcement depth ratios at e/B=0.16, α=15.

Table 3. Load carrying capacity improvement ratio (IR%) for various reinforcement first layer depths under various loading conditions.

e/B, α	U=0.25B	U=0.5B	U=0.75B	U=1B
0, 0	77.6%	70.6%	26.5%	2.9%
0.04, 5	64.9%	86.1%	53.6%	5.7%
0.08, 5	49.2%	72%	27%	5.8%
0.16, 5	69.9%	115.1%	53.4%	5.5%
0.04, 10	63.2%	73.2%	45.3%	10.5%
0.08, 10	63.2%	72.5%	20.9%	4.4%
0.16, 10	114%	126.5%	50.7%	1.4%
0.04, 15	79.4%	87.1%	29.4%	10.6%
0.08, 15	82.4%	93.7%	11.9%	3.8%
0.16, 15	117.3%	131.5%	15%	0%

In general, the outcomes reveal that the carrying capacity of the footing increases with reinforcing the soil with geogrid, and this increase reaches its maximum value at a depth ratio of U/B=0.50, which is the optimum depth of the first layer of reinforcement as shown in **Figs. 14 to 22** and given in **Table 3**. This value is similar to that found by **(AL-Saidi, 2009)** for the optimum value of U/B=0.50 for square footing under inclined load and that found by **(Al-Tirkity and Al-Taay, 2012)** for U/B=0.35-0.45 for strip footing under eccentric load.
It also can be noticed from the results how the footing carrying capacity decreases with increasing the depth ratio and that the reinforcement at (U/B=1) has a small or no impact on enhancing footing carrying capacity, and it's almost similar to unreinforced soil.

4. CONCLUSIONS

This study experimentally investigated the behavior of ring footing under eccentrically inclined load on treated and untreated sandy soil. After analyzing the outcomes of the tests, the following conclusions have been obtained:

- The carrying capacity of the footing decreases as the ring radius ratio increases due to the reduction in the effective area, and the optimum ring radius ratio under a combination of the eccentrically inclined load is n=0.30.
- The tilting of the footing increases as the eccentricity increases at the inclination angle of 15$^{o;}$ the percentage tilting is (3.4, 4.9, 7.9)% at (e/B=0.04, 0.08, 0.16), respectively.
- The horizontal displacement of the footing increases with increasing the inclination angle.
- The impact of the eccentricity is more significant than the impact of the inclination angle.
- Including the reinforcement increases the carrying capacity of the footing by (115.1%, 126.5%, and 131.5%) for (e=0.16 and α=5, 10, 15).
- The optimum depth ratio is when U/B is equal to 0.5, and the reinforcement layer with a depth ratio of U/B=1 almost has no improvement, and it's very similar to the unreinforced case.

REFERENCES

Al-Busoda, B.S., and Hussein, R.S., 2013. Bearing capacity of eccentrically loaded square foundation on compacted reinforced dune sand over gypseous soil. *Journal of earth sciences and geotechnical engineering,* 3(4), pp. 47-62.

Al-Jeznawi, D., and Al-Azzawi, A.A., 2021. The behavior of strip footing resting on soil strengthened with geogrid. Civil and Environmental Engineering, 17(2), pp. 597-609. Doi:10.2478/cee-2021-0060

Ali, A.M., 2016. Evaluation of bearing capacity of strip foundation subjected to eccentric inclined loads using finite element method. *Journal of Engineering*, 22(8), pp. 86-102. Doi:10.31026/j.eng.2016.08.06.

Al-Mhaidib, A.I., 1999. Bearing capacity of a model pile in sand under different loading rates. *The Ninth International Offshore and Polar Engineering Conference*.

Al-Mosawe, M.J., Al-Saidi, A.A., and Jawad., F.W., 2010. Bearing capacity of square footing on geogrid-reinforced loose sand to resist eccentric load. *Journal of Engineering*, 16(2), pp. 4990-4999.

Al-Mosawe, M.J., Al-Saidi, A.A., and Jawad, F.W., 2008. Improvement of soil using geogrids to resist eccentric loads. *Journal of Engineering*, 4(14), pp. 3198-3208.

AL-Saidi, A.A., 2009. Evaluation the behavior of reinforced loose sand under inclined loading. *Journal of Karbala University*, 7(3), pp. 98-108.

Al-Sumaiday, H.G.R., and Al-Tikrity, I.S.H., 2013. Experimental investigation of the bearing pressure for circular and ring footings on sand. *Tikrit Journal of Engineering Sciences*, 20(3), pp. 64-74. Doi:10.25130/tjes.20.3.07

Al-Tirkity, J.K., and Al-Taay, A.H., 2012. Bearing capacity of eccentrically loaded strip footing on geogrid reinforced sand. *Tikrit Journal of Engineering Sciences*, 19(1), pp. 14-22. Doi:10.25130/tjes.19.1.02

American Society of Testing and Materials (ASTM), 2006. Standard test method for classification of soil for engineering purposes (Unified Soil Classification System), ASTM D2487-06, West Conshohocken, Pennsylvania, USA.

American Society of Testing and Materials (ASTM), 1969. Standard Test Method for Relative Density of Cohesionless Soils, ASTM D 2049-69 International, West Conshohocken, Pennsylvania, USA.

American Society of Testing and Materials (ASTM), 2006. Standard Test Method for Particle Size-Analysis of Soils, ASTM D422-63 (2002), West Conshohocken, Pennsylvania, USA.

American Society of Testing and Materials (ASTM), 2006. Standard Test Method for Specific Gravity of Soil Solids by Water Pycnometer, ASTM D854, West Conshohocken, Pennsylvania, USA.

Bachay H.A., and Al-Saidi A.A., 2022. The optimum reinforcement layer number for soil under the ring footing subjected to inclined load. *Journal of Engineering*, 28(12), pp. 18-33. Doi:10.31026/j.eng.2022.12.02

Boushehrian, J.H., and Hataf, N., 2003. Experimental and numerical investigation of the bearing capacity of model circular and ring footings on reinforced sand. *Geotextiles and Geomembranes*, *21*(4), pp. 241-256. Doi:10.1016/S0266-1144(03)00029-3

Boushehrian, A. H., and Hataf, N., 2009. Bearing capacity of ring footings on reinforced clay. In *Geosynthetics in Civil and Environmental Engineering: Geosynthetics Asia 2008 Proceedings of the 4th Asian Regional Conference on Geosynthetics in Shanghai, China,* pp. 328-331.

Cicek, E., Guler, E., and Yetimoglu, T., 2012. Effect of reinforcement type and number on the load-settlement behavior of strip footings. *3rd International Conference on New Developments in Soil Mechanics and Geotechnical Engineering.*

Das, S.K., and Samadhiya, N.K., 2020. A numerical parametric study on the efficiency of prestressed geogrid reinforced soil. In *E3S Web of Conferences,* 205, P. 12004. Doi:10.1051/e3sconf/202020512004

El-Sawwaf, M., and Nazir, A., 2012. Behavior of eccentrically loaded small-scale ring footings resting on reinforced layered soil. *Journal of Geotechnical and Geoenvironmental Engineering*, 138(2), pp. 376-384. Doi:10.1061/(ASCE)GT.1943-5606.0000593

Fakher, N.A., and Fakhruldin, M.K., 2021. Influence of the number of reinforcement layers on the bearing capacity of strip foundation resting on sandy soil, *Al-Qadisiya Journal for Engineering* Science, 13, pp. 300-305. Doi:10.30772/qjes.v13i4.689

Fazel, S.A.H., and Bazaz, B., 2020. Behavior of eccentrically inclined loaded ring footings resting on granular soil. *International Journal of Engineering*, 33(11), pp. 2146-54. Doi:10.5829/IJE.2020.33.11B.04

Gupta, S., and Mital, A., 2021. Behaviour of eccentrically inclined loaded rectangular foundation on reinforced sand. *Studia Geotechnica et Mechanica*, 43(2), pp. 74-89. Doi:10.2478/sgem-2021-0003

Jawad, Z.H., and Shakir, R.R., 2021. Behavior of foundation rested on geogrid-reinforced soil: a review. In *IOP Conference Series: Materials Science and Engineering* (Vol. 1094, No. 1, p. 012110). IOP Publishing. Doi:10.1088/1757-899X/1094/1/012110

Kadhum, M.Q., and Al-Busoda, B.S., 2021. Behaviors of ring and circular footings subjected to eccentric loading: a comparative study. *IOP Conference Series: Materials Science and Engineering*, 1067(1), P. 012056. Doi:10.1088/1757-899X/1067/1/012056

Kolay, P.K., Kumar, S., and Tiwari, D., 2013. Improvement of bearing capacity of shallow foundation on geogrid reinforced silty clay and sand. *Journal of Construction Engineering*, *2013*, pp. 1-10. Doi:10.1155/2013/293809

Patel, P., and Bhoi, M., 2019. Study of Bearing Capacity and Settlement Behaviour of Solid Circular and Hollow Circular Footings on Granular Soil. *Proceedings of the 4th World Congress on Civil, Structural, and Environmental Engineering (CSEE'19) Rome, Italy – April*, Pap. No. ICGRE 163. Doi:10.11159/icgre19.163

Raheem, A.M., and Abdulkarem, M.A., 2016. Experimental testing and analytical modeling of strip footing in reinforced sandy soil with multi-geogrid layers under different loading conditions. *American Journal of Civil Engineering*, 4(1), pp. 1-11. Doi:10.11648/j.ajce.20160401.11

Sharma, V., and Kumar, A., 2018. Behavior of ring footing resting on reinforced sand subjected to eccentric-inclined loading. *Journal of Rock Mechanics and Geotechnical Engineering*, 10(2), pp. 347-357. Doi:10.1016/j.jrmge.2017.11.005

Shukla, S., Sivakugan, N., and Das, B., 2009. Fundamental concepts of soil reinforcement—an overview. *International Journal of Geotechnical Engineering*, *3*(3), pp. 329-342. Doi:10.3328/IJGE.2009.03.03.329-342

Snodi, L.N., 2010. Ultimate bearing capacity of ring footings on sand. *Wasit Journal for Science and Medicine*, 1, P. 7180.

Yadu, L., and Tripathi, R., 2013. Effect of the length of geogrid layers in the bearing capacity ratio of geogrid reinforced granular fill-soft subgrade soil system. *Procedia - Social and Behavioral Sciences*, 104, pp. 225-234. Doi:10.1016/j.sbspro.2013.11.115

Xu, C., Liang, C., Shen, P., and Chai, F., 2020. Experimental and numerical studies on the reinforcing mechanisms of geosynthetic-reinforced granular soil under a plane strain condition. *Soils and Foundations*, *60*(2), pp. 466-477. Doi:10.1016/j.sandf.2020.03.003